Monte Carlo study of semiflexible living polymers

Andrey Milchev[1] and D. P. Landau[2]
[1]*Institute for Physical Chemistry, Bulgarian Academy of Sciences, 1040 Sofia, Bulgaria*
[2]*Center for Simulational Physics, Department of Physics and Astronomy, The University of Georgia, Athens, Georgia 30602*
(Received 12 October 1994)

We study the order-disorder phase transition and the cluster-size distribution of "living polymers" in a lattice-hole model of a polydisperse system of semiflexible chain macromolecules by Monte Carlo simulation. In two dimensions we find that the transition line in T-μ space (temperature–chemical potential) contains a tricritical point and that the values of the critical exponents along the second-order portion of the phase boundary belong to the Ising universality class. In three dimensions a finite-size scaling analysis suggests that the phase transition is always first order. In both cases the chain lengths of the polymers follow an exponential probability distribution although the dependence of the mean chain length on density and temperature deviates from predictions of analytical theory.

PACS number(s): 61.25.Hq, 05.50.+q, 64.60.Cn

I. INTRODUCTION

Systems in which polymerization is believed to take place under condition of chemical equilibrium between the polymers and their respective monomers are termed "living polymers." These polymers are long linear-chain macromolecules that can break and recombine reversibly and so are in equilibrium with respect to their molecular weight distribution. A number of examples have been studied in recent years, including liquid sulfur [1–3] and selenium [4], poly(α-methylstyrene) [5], polymerlike micelles [6,7], and protein filaments [8].

The reversible aggregation of monomers into linear polymers exhibits critical phenomena which can be described by the $n \to 0$ limit of the n-vector model of magnetism [9,10]. Unlike mean field models, the n-vector model allows for fluctuations of the order parameter, the dimension n of which depends on the nature of the polymer system. (For linear chains $n \to 0$, whereas for ring polymers $n = 1$.) In order to study living polymers in solutions, one should model the system using the *dilute* $n \to 0$ magnet model [10]; however, theoretical solution presently exists only within the mean field approximation, where it corresponds to the Flory theory of polymer solutions [11]. For the case of semiflexible chains, Flory's model predicts a first-order phase transition between a low-temperature ordered state of stiff parallel rods and a high-temperature disordered state due to disorientation of the chains. An extension of the model to a system of self-assembling polymer chains [12] has been motivated by its relevance for the nature of the glass transition, and a number of simulational studies [13–15] have been carried out recently. However, the order of the phase transition lines has not been established unambiguously so far (most of these computer experiments were performed on two-dimensional lattices), and a number of scaling predictions [7], concerning the temperature and density dependence of the average chain length, have also not been addressed.

In the present work we use Monte Carlo methods to investigate the general features of the phase diagram of the model which was defined earlier [14]. With the aid of finite-size scaling, we determine the nature of the phase transition in both two and three dimensions. A comparison between scaling predictions [7] and simulational data for the equilibrium chain-length distribution confirms the expected exponential form of the probability distribution function (PDF), although the density and temperature dependence of the average chain length deviate from expected behavior.

II. MODEL

A detailed description of the model can be found in an earlier work [14], and here we only briefly summarize the main features. We consider regular L^D hypercubic lattices with periodic boundary conditions, where D is the spatial dimension. Each lattice site may either be empty or occupied by a (bifunctional) monomer with two strong (covalent) "dangling" bonds, pointing along separate lattice directions. These monomers fuse when dangling bonds of nearest-neighbor monomers point toward one another, releasing energy $v > 0$ and forming a backbone of self-avoiding polymer chains (no crossing at vertices). Right-angle bends, ensuring the semiflexibility of such chains, are assigned an additional activation energy $\sigma > 0$ in order to include the inequivalence between rotational isomeric states (e.g., *trans* and *gauche*) which is found in real polymers. The third energetic parameter w, reflecting the weak (van der Waals) *interchain* interactions, is responsible for the phase separation of the system into dense and sparse phases (with different density θ) when temperature T and/or chemical potential μ are changed. w is thus the work for creation of empty lattice sites (holes) in the system. One can define (cf. Table I) $q = 7$ possible states $\mathcal{S}_i$ of a monomer i on a two-dimensional (2D) lattice (two straight "stiff" junctions, $\mathcal{S}_i = 1,2$, four bends, $\mathcal{S}_i = 3, \ldots, 6$, and a hole $\mathcal{S}_7$), and $q = 16$ monomer states in a 3D cubic lattice. (This model can be mapped onto an unusual q-state Potts model and,

TABLE I. Possible states $\mathcal{S}_i$ of a monomer i on a 2D lattice.

1	2	3	4	5	6	7
—	|	L	⌜	⌝	⌟	

in fact, this representation was actually used for the simulation.)

The Hamiltonian for the model can then be written as

$$H=\sum_{i<j}\mathcal{J}_{ij}\mathcal{S}_i\mathcal{S}_j-\sum_i(\mu+\epsilon_i)\mathcal{S}_i\ , \tag{1}$$

where $|\mathcal{S}_i|=1$ for $\mathcal{S}_i=1,2,\ldots,6$, and $|\mathcal{S}_7|=0$ (a hole). It is important to note that the interaction constant depends on the mutual position of the nearest-neighbor monomer states, $\mathcal{J}_{ij}\neq\mathcal{J}_{ji}$. Thus, for example, $\mathcal{J}_{13}=-w$ whereas $\mathcal{J}_{31}=-v$. The local energies $\epsilon_i=\sigma$ for the bends and $\epsilon_i=0$ for the *trans* segments.

The ground states of this lattice model depend on the relative strengths of the three characteristic parameters v, w, and σ. Long chains at low temperatures are energetically favored only if $v/w>1$. In reality the v/w of covalent to van der Waals bond energies varies roughly from 10 to 100, and we have considered this entire range in our choice of our parameter values. As an example of the states which result from the simulation, in Fig. 1 we show a "snapshot" of a typical configuration in the disordered state for $D=2$. It is also clear that for $\sigma>0$ the chains will become stiffer with decreasing temperature and at temperature $T=0$ the ground state will be given by an orientally ordered array of parallel infinitely long rods, whereas for $\sigma=0$ disoriented chains will exist down to the lowest temperature [14]. Earlier [16] it has been shown that the long-range orientational order does not exist if the *intermolecular* interaction w is set equal to zero. Since the case of $w=0$ and $v\neq0$ has been considered elsewhere [17], in which the polymerization transition alone has been studied, in the present work we shall focus on the order-disorder transition in the case of all three parameters v, w, and σ different from zero.

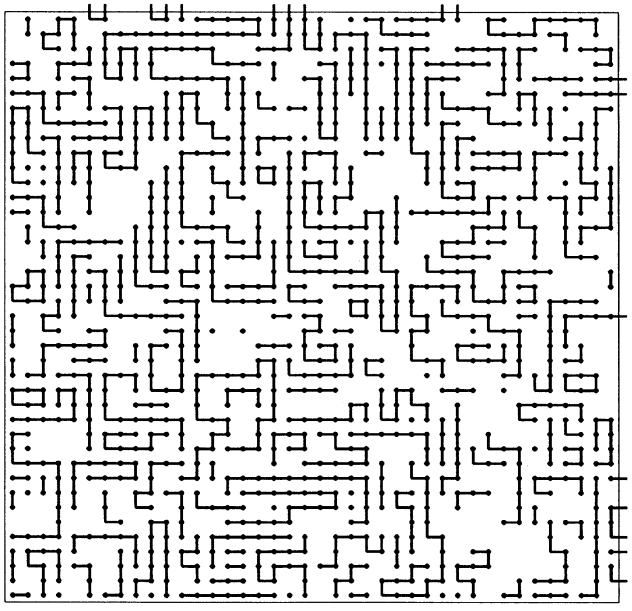

FIG. 1. A snapshot of a typical system configuration in the disordered state at $T=0.5$ after 2×10^5 MCS. Here $\sigma=0.5$, $v=2.0$, $w=0.1$, $\mu=-2.0$.

III. MONTE CARLO PROCEDURE

In our simulations we use a standard Metropolis method [18] with the number of Monte Carlo (MC) steps per site (MCS) depending on the system size and on the state point under consideration. For the systems described above, finite-size effects produce visible differences in the temperature dependence of all thermodynamic parameters for all lattice sizes that we could investigate. Because of difficulties with equilibration for large systems we restricted our study of thermodynamic properties to $L\leq14$ in both 2D and 3D. The length of the simulations in 2D was typically 5×10^4 MCS for equilibration and from 2.05×10^6 MCS for $L=6$ to 7.5×10^5 MCS for $L=14$ for calculating averages. Because of the larger number of sites in 3D, slightly shorter runs were used, e.g., 10^5 MCS for $L=10$.

For studies of the PDF of chain lengths far from criticality, however, typically a lattice size $L=60$ was used so that finite-size effects should be minimal. In our simulations we compute the orientational order parameter: in 2D $\Psi=|c_1-c_2|$ (here c_i denotes the concentrations of segments in the ith state), where c_1 and c_2 are the fractions of stiff *trans* segments pointing horizontally and vertically on the square lattice; in 3D we define an order parameter as $\Psi=\{[(c_1-c_2)^2+(c_1-c_8)^2+(c_2-c_8)^2]/2\}^{1/2}$, and c_1,c_2,c_8 are the fractions of *trans* bonds pointing in the x, y, and z directions.

We compute the order parameter susceptibility χ, the fourth-order "cumulant" $U=1-\langle\Psi^4\rangle/[3\langle\Psi^2\rangle^2]$, as well as the number of thermodynamic quantities, such as internal energy E, total density θ, specific heat C, compressibility $\kappa=(L^2/k_BT^2)(\langle\theta^2\rangle-\langle\theta\rangle^2)$, and the average flexibility of the chains $f=(1-c_1-c_2)/(1-c_0)$, which is given by the ratio of the number of bends over the total number of monomers (c_0 is the concentration of vacancies in the lattice). Since polymer chains may, in principle, form rings, in addition to the PDF of chain lengths and the average chain length, the average number of rings is also calculated.

IV. RESULTS: TWO-DIMENSIONAL LATTICES

A. Phase diagram

We have performed our simulations at various values of the characteristic interactions, although most of the work was done for $v=2.0$, $w=0.1$, and for both comparatively flexible, $\sigma=0.5$, and stiff, $\sigma=2.0$, chains. The critical chemical potential at $T=0$ is $\mu_c=-(v+w)$, below which the lattice is completely empty. At finite temperature due to the nonzero values of the parameters w,v,σ, the formation of long semiflexible chains couples to vacancy creation in the system, and to a simultaneous stiffening of the chains, so that the polymerization transition "drives" also a transition from lower to higher density as well as a transition from a disordered into an ordered state [14].

The resultant phase diagram for $v=2.0$, $w=-0.1$ is shown in Fig. 2(a) for two different values of σ. In both cases the transition is first order at low temperatures, but above a tricritical point $T_t=0.3$ the transition becomes second order. The first-order line on our phase diagram separates "dense" from the "rare" polymer solution, and the polymerization transition occurs along the entire order-disorder phase boundary which in 2D includes both first-order and second-order parts. As Fig. 2(a) shows, we find that the transition line for stiff chains rises more steeply as the chemical potential is increased than for the more flexible chains, and the asymptotic critical temperature is much higher. While for $\mu>\mu_c$ the density is quite high in both the ordered phase as well as the high-temperature disordered phase, for $\mu<\mu_c$ the lattice is virtually empty up to a temperature (the Lifshitz line) at which a rather steep increase in θ is accompanied by pronounced maxima in the second derivatives of the thermodynamic potentials. Although this line does not mark a real phase transition, it separates a high-temperature region of structured disordered phase (cf. Fig. 1) from that of a very dilute disordered phase at low T. The partial alignment of chains is indeed evident in Fig. 1, with a well defined characteristic wavelength which results in a peak at a nonzero wave vector in the structure factor [19].

The nature of the transition along the second-order portion of the boundary can be extracted using finite-size scaling. Such an analysis was carried out for different values of chemical potential μ; typical data for the temperature variation of some thermodynamic quantities with $\mu=-1.4$, and the respective scaling plots, are shown in Fig. 3.

Usually the critical temperature of the phase transition, T_c, may be determined from the crossing point of the cumulant curves which, depending on the lattice size L, decay more or less steeply from $U=\frac{2}{3}$ at $T=0$ to $U=0$ at $T\to\infty$. The data for a flexible chain system ($\sigma=0.5$) are plotted in Fig. 3. All of the lattice sizes cross quite close together, i.e., $T_c=0.390\pm0.002$, with a value of $U^*=0.625\pm0.010$, which is consistent with the 2D Ising value.

With T_c thus known, a scaling plot of U yields the critical index ν when all curves collapse onto a single master

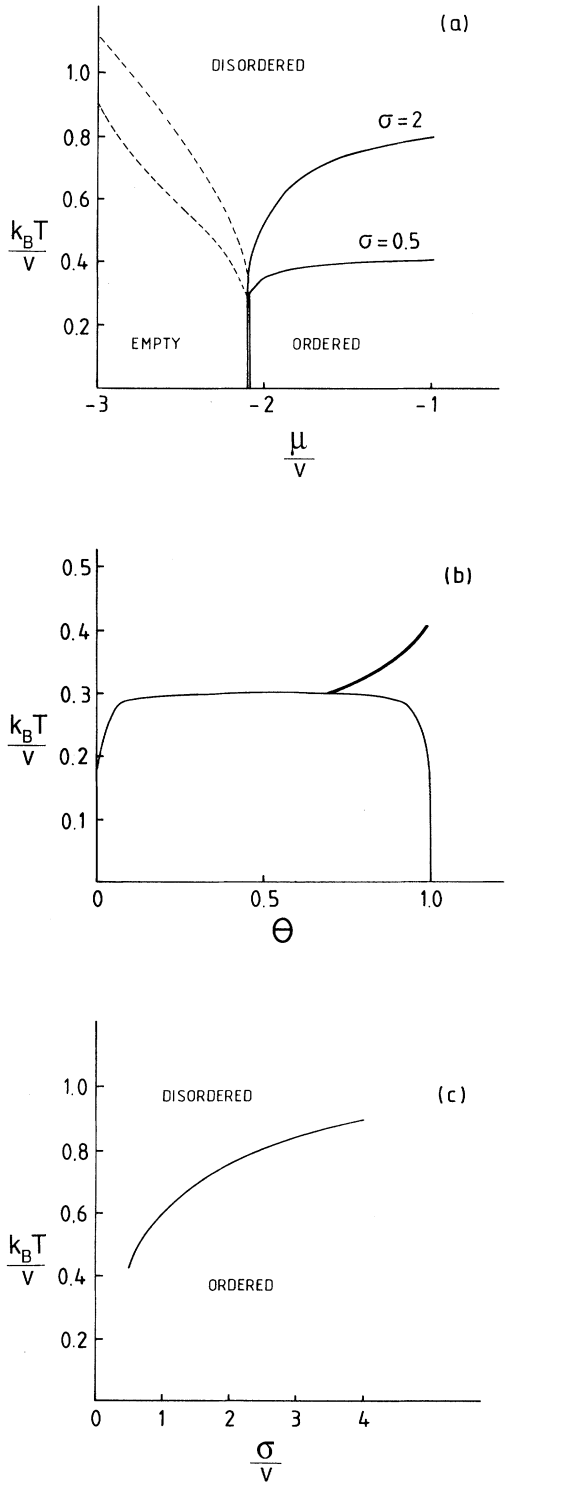

FIG. 2. Phase diagram of the 2D system for $v=2.0$, $w=0.1$: (a) T_c as a function of chemical potential μ for two values of the rigidity parameter σ. The single line indicates a second-order phase transition between disordered and ordered phases, the double line denotes first-order transition, and dots mark the Lifshitz line. (b) T_c as a function of coverage θ for $\sigma=0.5$. (c) Variation of the critical temperature for polymerization, T_c, with the rigidity parameter σ for $\mu=-1.4$.

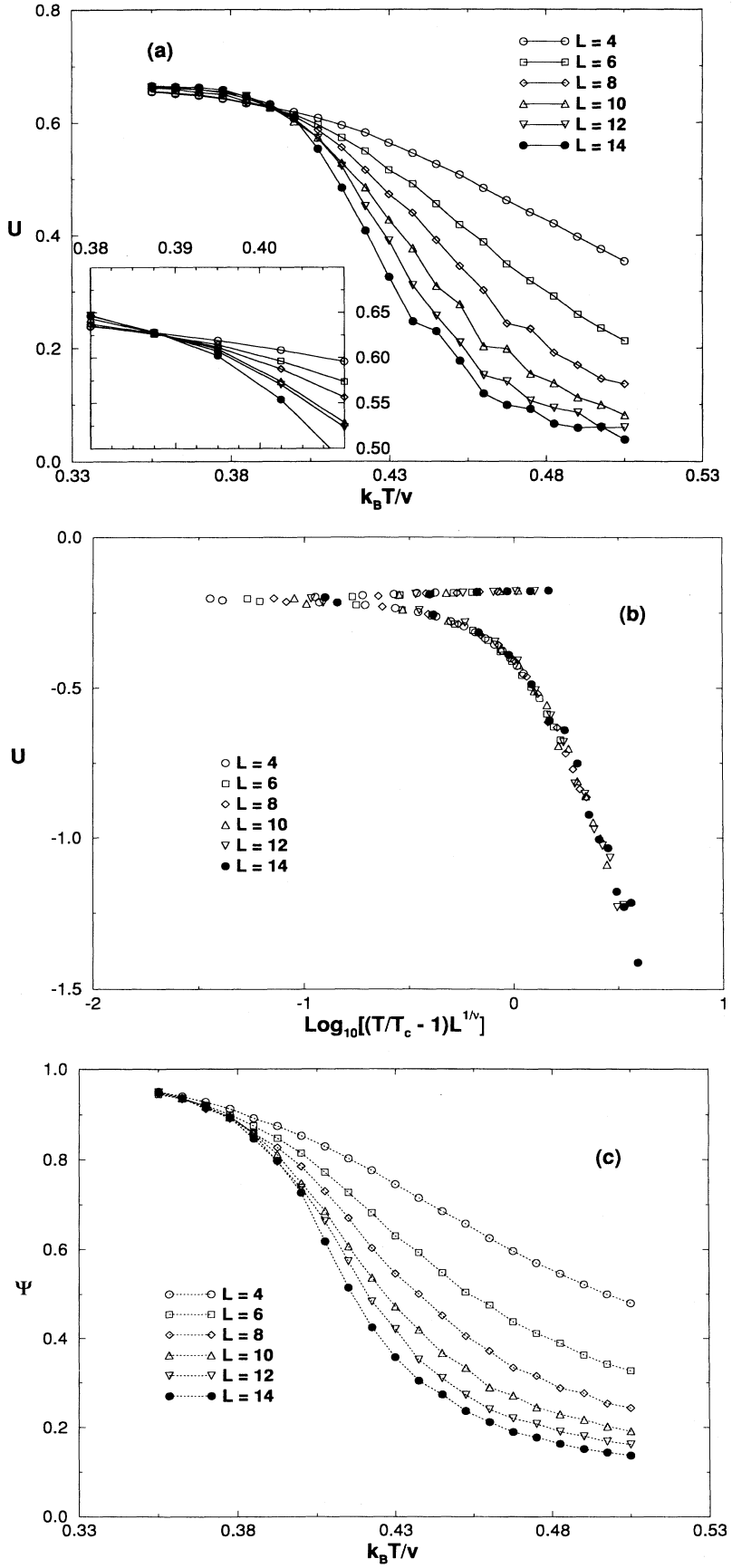

FIG. 3. Temperature dependence of thermodynamic quantities in the vicinity of the polymerization transition in 2D with $\sigma=0.5$, $v=2.0$, $w=0.1$, and $\mu=-1.4$, and for various lattice sizes L as shown: (a) The fourth-order "cumulant" U. The inset shows the immediate vicinity of the cumulant crossing using a magnified scale. (b) Scaling plot of the same data as (a). (c) Order parameter Ψ. (d) Scaling plot with $T_c=0.390$, $\nu=1.0$, and $\beta=0.125$. (e) Susceptibility χ. (f) The same data as (e) in scaling form.

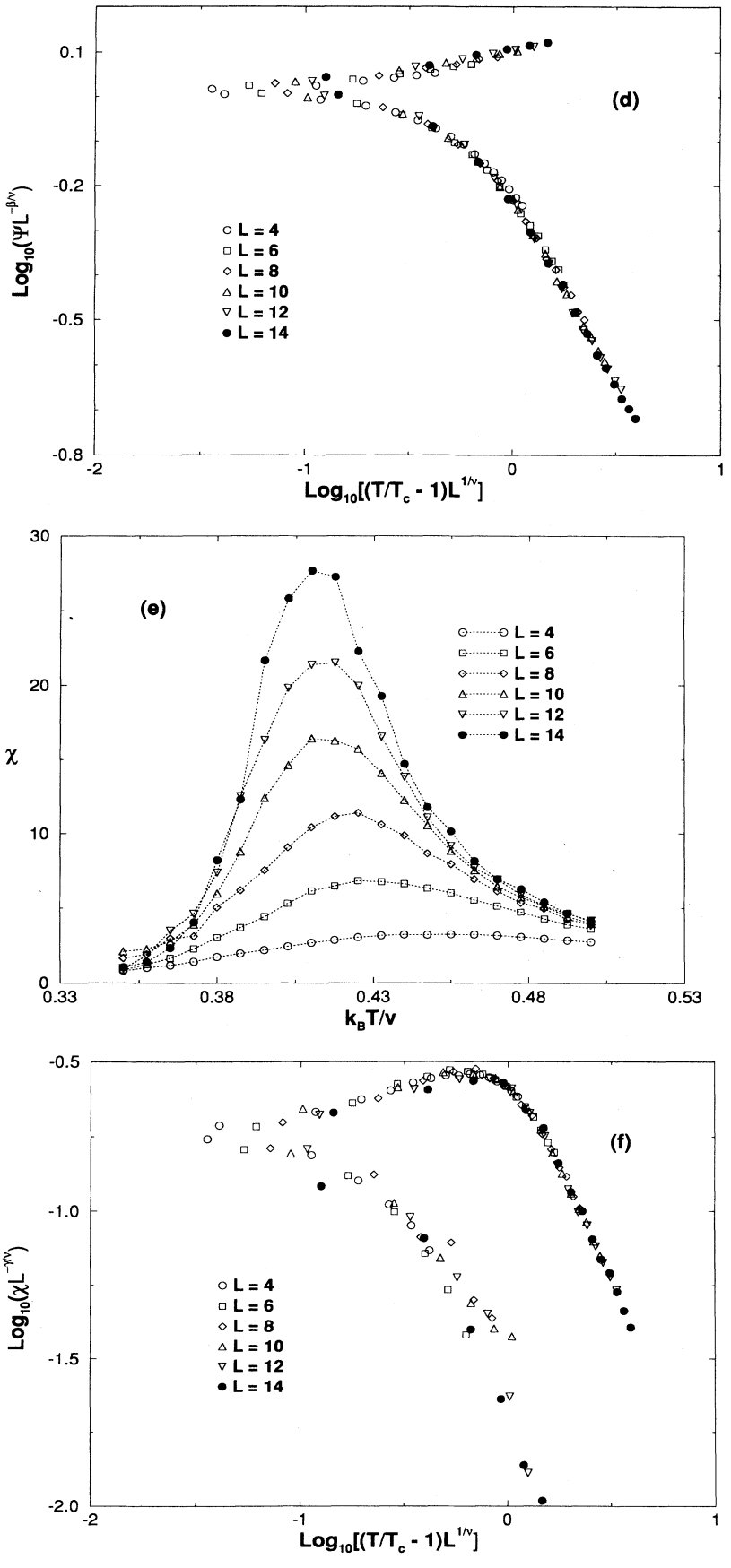

FIG. 3. (*Continued*).

curve [cf. Fig. 3(b)]. With both T_c and ν thus determined, other critical indices may be evaluated from the scaling plots of the respective thermodynamic quantities.

It is evident from Figs. 3(c) and 3(d) that the order parameter scales fairly well with the Ising values of the critical indices, $\nu=1$ and $\beta=0.125$. The scaling of the susceptibility, χ, is somewhat worse in the subcritical branch of the master curve, which is probably due to long correlation lengths and slow equilibration in the ordered state. Very similar scaling behavior is observed for the case of stiff chains, $\sigma=2$, and for different values of μ (the plots are not shown here). We believe that this behavior clearly demonstrates that in 2D the second-order portion of the phase diagram for equilibrium polymerization belongs to the Ising class of universality. This result could perhaps be anticipated since the ordered state, consisting of infinitely long rigid parallel rods, is doubly degenerate on the square lattice. It is thus to be expected that the type of lattice would affect the universality class of the transition line (e.g., on a triangular lattice it would be that of a $q=3$ Potts model).

In Fig. 2(b) we also show the phase diagram in coverage-temperature space. Here, the first-order portion of the phase boundary shown in Fig. 2(a) has opened up into a large coexistence region leaving only a relatively small area of the pure ordered phase. The shape of this phase diagram is quite similar to that predicted by Kennedy and Wheeler [3], including the asymmetry of the coexistence region. In Fig. 2(c) we show the variation of the critical temperature with σ; as the chains become stiffer, T_c rises monotonically.

B. Chain length distribution

As pointed out by Flory [11], the principle of equal reactivity, according to which the opportunity for reaction (fusion or scission) is independent of the size of the participating polymers, implies an exponential decay of the number of polymers of size l as a function of l. Indeed, at the level of mean-field approximation in the absence of closed rings, one can write the free energy for a system of liner chains [7] as

$$\frac{F}{k_B T}=\sum_l P(l,T)\left[\ln P(l,T)+\frac{v}{k_B T}\right], \tag{2}$$

where the PDF for chain length l is denoted by $P(l,T)$ and k_B stands for the Boltzmann constant. The density of the system, θ, is then

$$\theta=\sum_l lP(l,T)\ . \tag{3}$$

Minimization of Eq. (2) with respect to $P(l,T)$, subject to the condition Eq. (3), yields

$$P(l,T)\propto\exp\left[-\frac{l}{l_{\rm av}}\right], \tag{4}$$

$$l_{\rm av}\simeq\theta^{1/2}\exp\left[\frac{v}{2k_B T}\right]. \tag{5}$$

This result should be valid for sufficiently high-density θ where correlations, brought about by the mutual avoidance of the chains, are negligible. In Fig. 4 we show a semilogarithmic plot of the PDF for chain lengths, $P(l,T)$, at various temperatures and verify that the predicted exponential dependence on l is nicely fulfilled. At low temperatures, $T=0.35$–0.45, there are also visible oscillations in $P(l,T)$ at small chain lengths, $l\leq 20$, whereby even oligomers occur more frequently than odd ones. This effect appears to reflect the fact that short cyclic chains are energetically favored and is an artifact of the square lattice. The density dependence of the mean length $l_{\rm av}$ however, deviates from the predictions. While the mean-field result, Eq. (5), predicts $l_{\rm av}\propto\theta^{1/2}$, a scaling theory analysis suggests for the case of semidilute solution of chains [7],

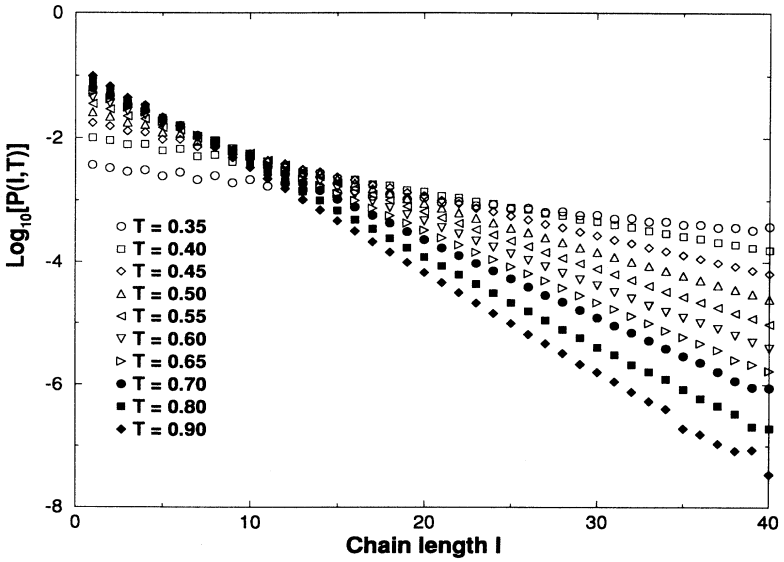

FIG. 4. Semilogarithmic plot of the probability distribution function $P(l,T)$ vs chain length l in the disordered regime at different temperature T (given as a parameter) for $D=2$. Here $\sigma=0.5$, $v=2.0$, $w=0.1$, and $\mu=-2.0$.

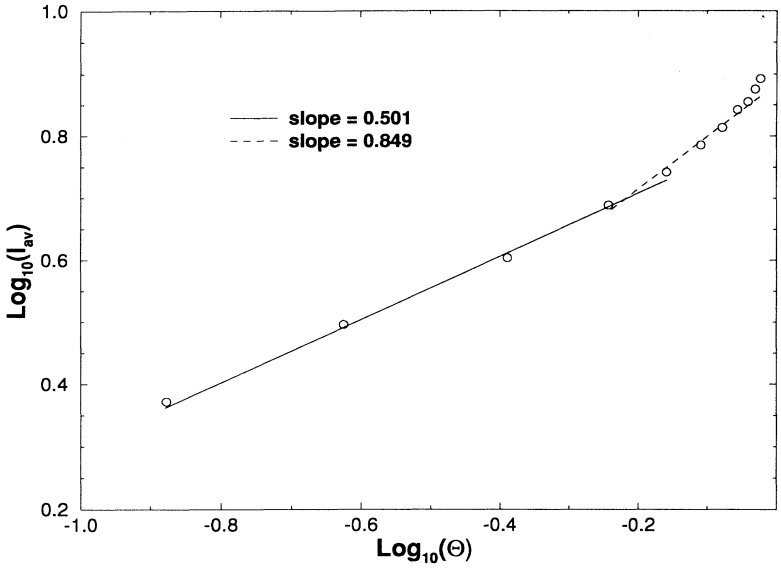

FIG. 5. Log plot of the dependence of mean chain length l_{av} on total density θ for $D=2$. The slopes far from and near to the critical region are given by dashed and solid lines, respectively.

$$l_{av} \propto \theta^{y} \exp\left[\frac{v}{2k_B T}\right], \tag{6}$$

with

$$y=\frac{1}{2}\left[1+\frac{\gamma-1}{\nu(D-1)}\right] \tag{7}$$

where in two dimensions, $D=2$, and with the critical exponents for self-avoiding walks [20], $\gamma=\frac{43}{32}$, $\nu=\frac{3}{4}$, one has $y\simeq 0.843\,75$. It is clear from Fig. 5 that over a broad range of density the power $\frac{1}{2}$ may be observed, whereas at higher density instead of slope y the measured values of $\ln(l_{av})$ show a distinct curvature which happens immediately at the phase transition line. Although our model allows the formation of rings, and we actually observe them in the simulations, they occur comparatively seldom and could hardly be responsible for the observed discrepancy.

The dependence of the mean length l_{av} on inverse temperature T^{-1}, shown in Fig. 6, demonstrates that the actual l_{av} vs T relationship appears to be clearly of non-Arrhenius type. Thus the expected slope $v/2=1$, which is marked by a dashed line on the plot, holds on the average only.

V. RESULTS: THREE-DIMENSIONAL LATTICES

When simulating the system on a cubic lattice one should bear in mind that a triple degeneracy of the ground state exists with the parallel rods pointing along any of the three Cartesian axes. Moreover, a sort of a smectic ordered state with each plane perpendicular to some axis containing ordered parallel rods will be formed at low temperature if the *interchain* interaction w be-

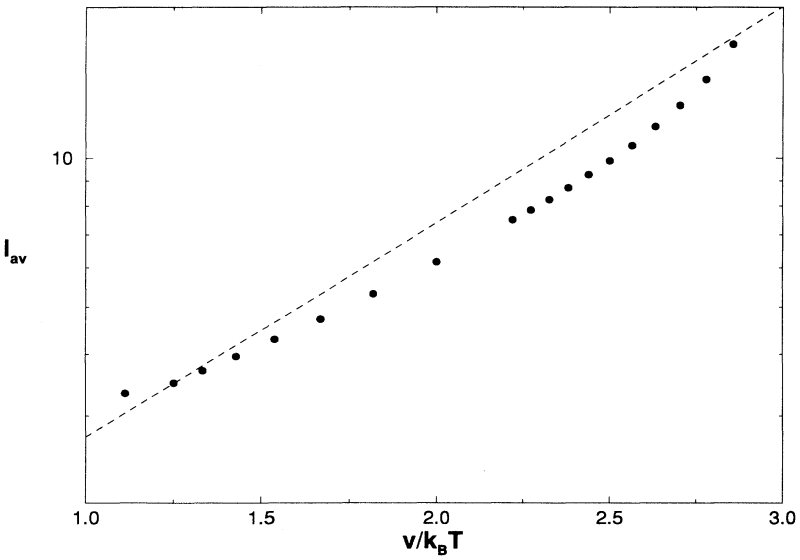

FIG. 6. Dependence of the mean chain length l_{av} for $D=2$ on inverse temperature in semilogarithmic coordinates.

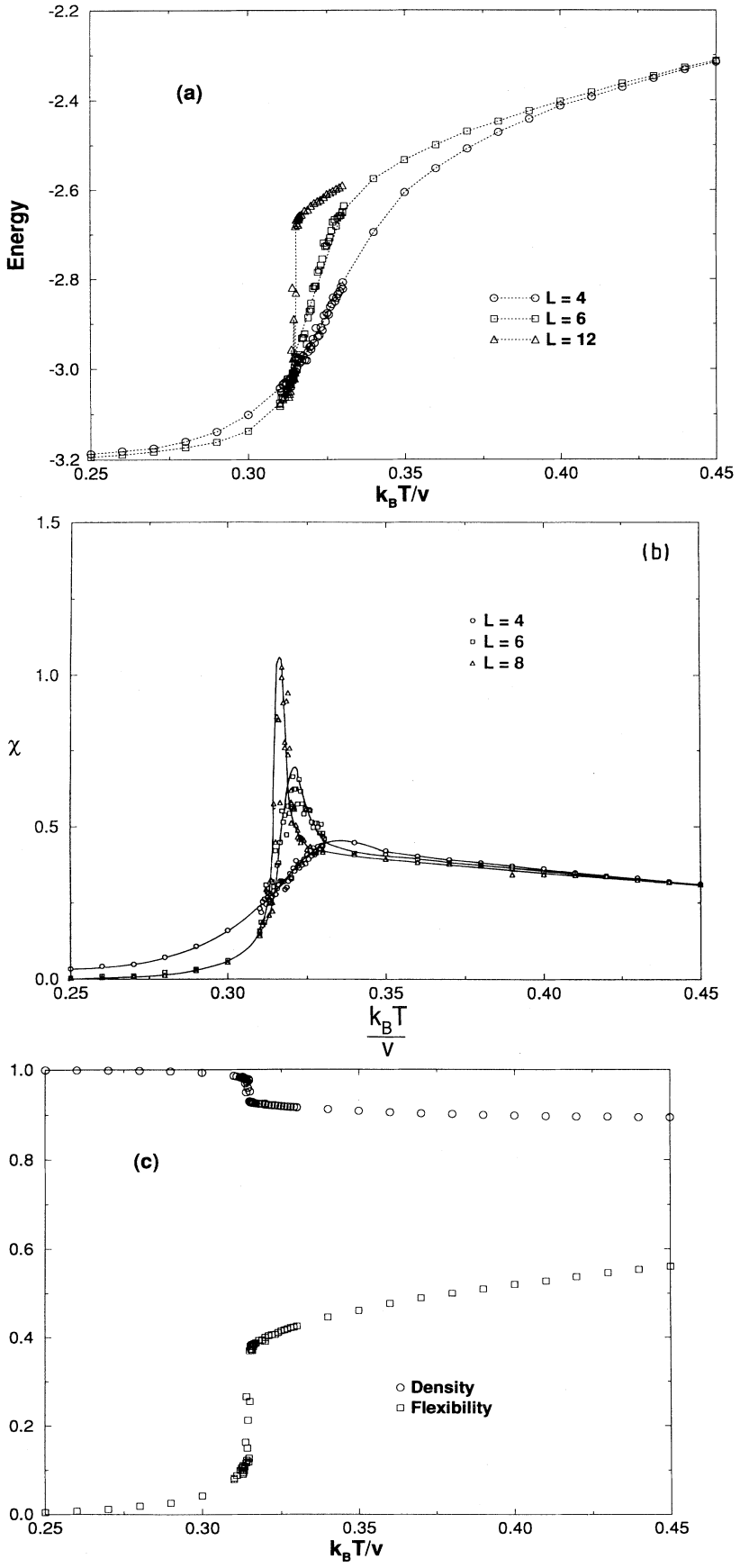

FIG. 7. Dependence of thermodynamic quantities on temperature in 3D: (a) Internal energy of a system with lattice size $L=4$, 6, and 12. Susceptibility for the same lattice sizes. (c) Total density (circles) of the system and average flexibility of the polymer chains (squares) for $L=12$. The interactions are identical to those of Fig. 4.

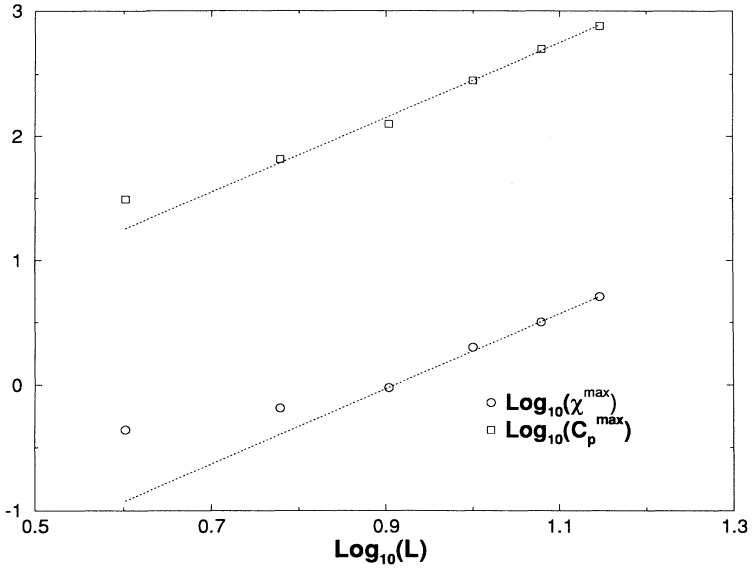

FIG. 8. Variation of the maxima of the specific heat (squares) and the susceptibility (circles) with lattice size L for $D=3$. Both dotted lines have slope 3.

tween nearest-neighbor monomers does not differentiate between pairs of rods which are parallel (in plane) or which cross at right angles when they belong to neighboring planes. Viewing the nearest-neighbor energy bonds as rough substitutes for the integral effect of longer range interactions, one could assume that the w's in both cases would differ so that in the former case (parallel rods) $w_{\parallel}$ is somewhat stronger than the latter one, $w_{\perp}$. Such an assumption leads to a ground state consisting only of stiff chains, parallel to one of the three axes, whereby the order parameter in 3D, defined in Sec. IV, attains a value of unity in the ordered state. In our simulations we have studied both $w_{\perp} \neq w_{\parallel}$ and $w_{\perp}=w_{\parallel}$, and find that for both cases the order-disorder transition turns out to be first order (Fig. 7). For small systems the behavior is rather smooth, but for lattices of size $L \geq 12$ an abrupt change in the thermodynamic quantities of the system is observed, reflecting a transition from a dense state of rigid parallel chains to a less dense disordered state (a melt) of chains with a great fraction of bends. The strongest evidence for the first-order nature of the phase transition can be obtained from the finite-size scaling behavior of quantities, such as the specific heat (C) or the susceptibility (χ) maxima at the transition temperature. It is well known [18] that for a first-order transition such quantities should scale as $\propto L^D$. Such behavior is indeed demonstrated in Fig. 8, where the slopes of the data for sufficiently large L are equal to 3. The phase diagrams in 3D, in both T-μ and T-θ spaces are shown in Fig. 9. The coexistence region is asymmetric and a pure, ordered phase exists only for a very small region of high densities. Superficially, the phase diagram μ-T space in 3D resembles that for 2D, but in θ-μ space the region of pure ordered phase is even further compressed.

The PDF of chain lengths in the cubic lattice is shown in Fig. 10 for several temperatures above and below the transition temperature $T_c=0.38$. Qualitatively, it is not different from that in 2D, complying with the form of Eq. (4). It turns out, however, that the average chain length in the disordered regime above the transition temperature is rather small, $l_{\mathrm{av}} \approx 2-3$, independent of the size of the lattice. On the contrary, in 2D, where the transition is

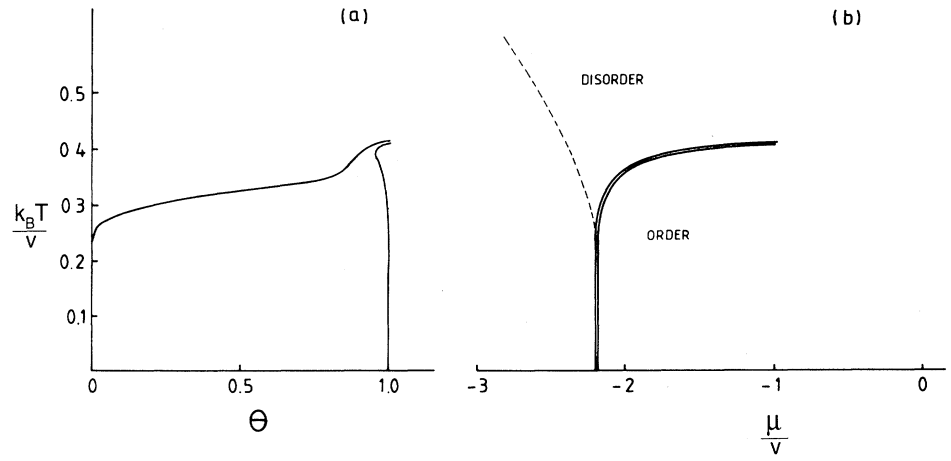

FIG. 9. Phase diagram for the 3D system: (a) T_c as a function of coverage θ; (b) T_c as a function of chemical potential μ.

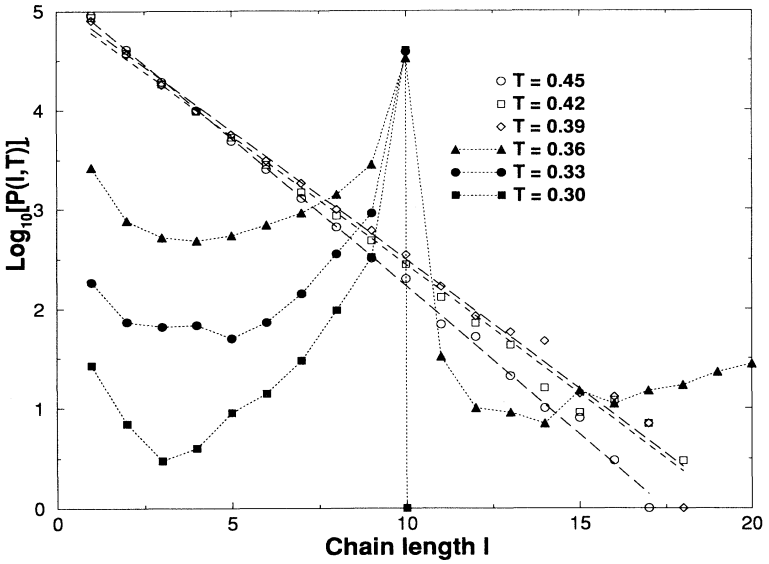

FIG. 10. Probability distributions of chain length above (dashed lines) and below the phase transition temperature in a $D=3$ lattice with $L=10$.

continuous, the average chain length always matches, and sometimes even exceeds, the lattice size L as the critical temperature is approached. It thus appears that the occurrence of long chains in 3D is a relatively rare event, even immediately at the phase transition line, although the density changes thereby little.

The eventual formation of a sharp single-peaked PDF below T_c is illustrated in Fig. 10 as well. One should bear in mind, however, that for these data the system has not reached thermal equilibrium yet, so they merely reflect the relaxation of the exponential form, Eq. (4), into a δ-like distribution, characterizing the ordered state.

VI. CONCLUSIONS

In summary, we have determined the phase diagrams for order-disorder transitions in a simple model for living polymers. Due to the temperature-dependent flexibility of the chains, as well as to the presence of *intrachain* and *interchain* forces, as long as this transition is first order it takes place simultaneously with a "rare-dense" polymer solution transition, and with a drastic change in the degree of polymerization. In 2D the phase boundary has a tricritical point and the second-order portion of the boundary belongs to the Ising universality class. In 3D the transition appears to be first order for all values of the chemical potential. An interesting feature of the phase diagrams which is found in both 2D and 3D is the existence of a Lifshitz line which separates the higher-temperature region of structured disordered phase from the region of ordinary disordered phase at low temperature. In this sense our system is similar to binary and ternary mixtures containing surfactants [19].

The probability distribution function of chain lengths in the state of disorder is found to have the expected exponential form. The average chain length dependence on temperature and density, however, although qualitatively in line, shows definite discrepancies with both mean field and scaling theory predictions. In our opinion this cannot be attributed alone to the presence of closed ring macromolecules, observed in the simulations, and it is hardly due to the model adopted in the present computer experiment. Clearly more work will be needed before the adequacy of the theoretical description is fully established.

ACKNOWLEDGMENTS

Technical assistance and helpful conversations with A. Ferrenberg, M. Laradji, and H.-G. Evertz are gratefully acknowledged. This research was supported by National Science Foundation Grants Nos. Int. 9304562 and DMR-9405018.

[1] R. L. Scott, J. Phys. Chem. **69**, 261 (1965).
[2] J. C. Wheeler, S. J. Kennedy, and P. Pfeuty, Phys. Rev. Lett. **45**, 1748 (1980).
[3] S. J. Kennedy and J. C. Wheeler, J. Phys. Chem. **78**, 953 (1984).
[4] G. Faivre and J. L. Gardissat, Macromolecules **19**, 1988 (1986).
[5] K. M. Zheng and S. C. Greer, Macromolecules **25**, 6128 (1992).
[6] J. Appel and G. Porte, Europhys. Lett. **12**, 185 (1990).
[7] M. E. Cates and S. J. Candau, J. Phys. Condens. Matter **2**, 6869 (1990).
[8] F. Oozawa and S. Asakura, *Thermodynamics in the Polymerization of Proteins* (Academic, New York, 1975).
[9] P. G. DeGennes, Phys. Lett. **38A**, 339 (1972); J. des Cloiseaux, J. Phys. **36**, 281 (1975).
[10] J. C. Wheeler and P. Pfeuty, Phys. Rev. A **24**, 1050 (1981).
[11] P. J. Flory, *Principles of Polymer Chemistry* (Cornell Uni-

versity Press, Ithaca, 1953).
[12] A. Milchev and I. Gutzow, J. Macromol. Sci. B **21**, 583 (1982).
[13] G. F. Tuthill and M. Jaric, Phys. Rev. B **31**, 2981 (1985).
[14] A. Milchev, Polymer **34**, 362 (1993).
[15] G. I. Menon, R. Pandit, and M. Barma, Europhys. Lett. **24**, 253 (1993).
[16] A. Baumgärtner, J. Chem. Phys. **84**, 1905 (1986).
[17] Y. Rouault and A. Milchev, Phys. Rev. E **51**, 5905 (1995).
[18] See, e.g., *Monte Carlo Methods in Statistical Physics,* edited by K. Binder (Springer-Verlag, Berlin, 1979).
[19] M. Laradji, H. Gou, and M. J. Zuckermann, J. Phys. Condens. Matter **6**, 2799 (1994).
[20] P. G de Gennes, in *Scaling Concepts in Polymer Physics* (Cornell University Press, Ithaca, 1979), Chap. 1